Engineering Structures 351 (2026) 121991

Contents lists available at ScienceDirect

Engineering Structures

journal homepage: www.elsevier.com/locate/engstruct

Testing timber columns for resistance until fire burnout: Role of thermal wave, smoldering, and active suppression

Thomas Gernay [a,*], Chenzhi Ma [a], Silvio Renard [b], Jean-Marc Franssen [c], Jochen Zehfuß [d], Robert McNamee [e], Patrick Bamonte [f], Fabienne Robert [b]

[a] Johns Hopkins University, Baltimore, USA
[b] CERIB Fire Testing Centre, Epernon, France
[c] Liege University, Belgium
[d] Technische Universität Braunschweig, Germany
[e] RISE, Research Institutes of Sweden, Sweden
[f] Politecnico di Milano, Italy

ARTICLE INFO

Keywords:
Natural fire tests
Timber columns
Glued-laminated timber (GLT)
Structural failure
Cooling phase
Burnout resistance
Thermal wave
Smoldering

ABSTRACT

This paper presents a numerical and experimental study on stability until burnout of glued-laminated timber columns in compartment fires. In a previously reported experimental study, six 3.7 m long, 280 × 280 mm^2 timber columns designed for 60 min of standard fire resistance failed to survive various compartment fires, with four of the six columns failing due to thermal wave penetration into the cross section during the decay phase of the fire. Here, six additional compartment fire tests are conducted, supported by numerical simulations, to investigate the design of timber columns for burnout resistance. A finite element model is used to design the size of the columns to mitigate the effect of the thermal wave. Five tests on columns up to 400 × 400 mm^2 show that increasing the section size at constant loading enhances fire endurance, but the columns later failed due to local smoldering. While failure in the smaller columns was driven by the thermal wave and occurred within two hours of ignition, failure in the larger columns was caused by smoldering and occurred more than 10 h after ignition. In a sixth test, on a 280 × 280 mm^2 column, water-based fire suppression was used 35 min after ignition. The column remained stable until burnout, showing that early fire suppression may prevent failure of timber columns by addressing both the thermal wave and smoldering mechanisms.

1. Introduction

Timber is increasingly being adopted as a primary structural material in modern buildings, driven by embodied carbon reduction goals and enabled by innovations in engineered wood products such as glued-laminated timber (GLT) and cross-laminated timber (CLT) [1,2]. These products enable long spans and high load capacities, making timber suitable for mid- and high-rise buildings [3]. Given this trend, concerns about fire safety are gaining renewed attention, particularly the ability of timber elements to maintain load-bearing capacity during and after fire exposure [4–6]. Standard fire resistance ratings offer a limited view, as they do not capture the behavior of structures exposed to natural fire development and decay. There is increasing recognition that performance-based design that considers the structural behavior throughout the entire fire event is necessary to evaluate the structural fire safety, especially in tall buildings where fire suppression may be delayed or limited [7,8].

Previous fire studies on timber structural members relying on standardized fire curves such as ISO 834 [9] aimed to assess whether the members can resist failure for a specified duration in standardized conditions, which provides useful benchmarks and underpins prescriptive fire design methods [10]. However, these studies do not interrogate the performance of timber members during the different phases of a real fire. According to Paragraph A7 in the new ISO 834 standard [9] "*The actual performance achieved in a fire resistance test is solely related to the test conditions.*" where the test conditions according to the standard do not include a cooling phase. The behavior of timber in fire is complex, involving pyrolysis, combustion, smoldering, thermal degradation, moisture migration, and delayed internal heating [11–13]. Additionally, mass timber members may experience char fall-off or delamination [14,

* Corresponding author.
E-mail address: tgernay@jhu.edu (T. Gernay).

https://doi.org/10.1016/j.engstruct.2025.121991
Received 28 August 2025; Received in revised form 9 December 2025; Accepted 20 December 2025
Available online 29 December 2025

15], and the type of adhesive influences the fire performance [16]. The thermal response of the section is at the base of the degradation of strength and stiffness which progressively reduces the load bearing capacity of the structural member. Several recent full-scale fire tests on structures with exposed mass timber have highlighted vulnerabilities during the decay phase of the fire. Most of these tests used unloaded timber members and focused on the fire dynamics, investigating issues of fire dynamics in large compartments [17–19], self-extinction [20], and smoldering (including behind encapsulation [21]). In contrast, the authors, focusing on structural burnout resistance, conducted both furnace tests [22] and natural fire tests [23,24] on loaded timber members, which highlighted delayed failure due to the thermal wave effect during the decay phase of the fire. Numerical studies also described these mechanisms of delayed thermal wave and accompanying reduction of strength and stiffness in the internal parts of the section [5,25].

In a previous study [24], the authors conducted six full-scale compartment fire tests on 3.7 m long, 280 × 280 mm² columns designed for 60 min of fire resistance. The fire conditions varied in opening factor, fire load, and wood crib configuration. All columns failed, with failure times ranging from 35 to 71 min. Notably, four of the six failures occurred after the fire had entered the decay phase. These experiments showed that timber columns can experience delayed failure driven by internal heat conduction even after cessation of flaming, a mechanism not captured by standard fire resistance ratings. Building on these experiments, there is a need to further explore the factors that influence column stability throughout the decay phase and to develop design approaches for burnout resistance in real fires.

This study investigates the conditions to achieve burnout resistance of load-carrying timber columns. Specifically, six new full-scale compartment fire tests are performed in which an increase in cross-section size and active fire suppression are considered. To guide the design of the new tests, finite element models were first developed and validated using data from the previous experiments [24]. These simulations were then used to select column sizes expected to resist failure caused by the thermal wave mechanism. By linking experimental observations with numerical modeling, the study advances understanding of how column size and active suppression influence failure mechanisms during the decay phase of natural fires. A key novelty of the work is that it provides results from natural fire experiments on loaded timber members designed specifically with the objective to achieve burnout resistance. The results of this research support the development of performance-based fire design strategies that move beyond standardized fire resistance ratings, to provide methods for more reliable and resilient fire design of mass timber structures.

2. Summary of the previous experiments on timber columns

2.1. Timber column specimens

As part of this research project, twelve identical timber columns were previously tested under various fire conditions [22,24]. The columns, with cross-sectional dimensions of 280 × 280 mm², were made of glued-laminated timber (GLT) from 40 mm thick spruce slats glued with MUF (Akzo Nobel System MUF 1247 / 2526 / 4426 “GripPro”). The strength and stiffness properties were provided by the manufacturer as those for GL 24 h [26]. The timber columns were 3680 mm long, with steel plates screwed at both ends for the connections, for a total length of 3740 mm between the axes of the supports, which were hinged-hinged (pinned-pinned) in one direction and restrained by the stiffness of the loading structure in the other direction. Type K thermocouples were placed in the columns at various depths.

The columns were subjected to an axial compressive load of 322 kN with an eccentricity of 20 mm in the direction of the hinge. This load was obtained based on Eurocode load combinations [27] considering a column representative of a five-story building with a fire resistance requirement of 60 min. The 322 kN load represents 100 % of the design capacity in fire situation of the column based on a charring rate of 0.70 mm/min and a 14 mm zero-strength layer per prEN 1995–1–2 [28], and 40 % of the design capacity at ambient temperature (refer to Gernay et al. [22] for more details on the column design).

2.2. Furnace tests

Six timber columns were tested in a standard furnace [22]. Two columns were exposed to ISO 834 heating until failure, with recorded fire resistance times of 55 and 58 min. Another two columns underwent 15 min of ISO 834 heating followed by controlled cooling at −10.4 °C/min; both failed during cooling, at 98 and 153 min, respectively. These delayed failures were caused by a sustained rise in internal temperatures persisting for several hours after peak gas temperatures, as shown by thermocouple data, leading to progressive loss of strength and stiffness in the columns. The last two columns, which were subjected to 10 min of ISO 834 heating followed by cooling at the same controlled rate of −10.4 °C/min, remained stable until the end of the test, when the displacements had stabilized and the internal temperatures had started to decrease. The furnace experiments showed that loaded timber columns may fail in the decay phase after exposure during a period corresponding to 25 % of their standard fire resistance time.

2.3. Compartment fire tests

Six compartment fire tests (labeled Tests 9, 10, 11, 14, 15, 17) were then conducted on identical specimens to investigate the response of the timber columns under natural fire [24]. The compartment measured 6.00 × 4.00 m at the floor level, as shown in Fig. 1. The ceiling height was 3.10 m for Tests 9 and 10, and 3.05 m for subsequent tests due to further protection with 55 mm of mineral wool after the first two compartment tests. Wood cribs were used as fuel, see Fig. 2. The columns were subjected to the same axial loading (322 kN) as in the furnace tests, with the load maintained during the whole fire duration. The tests vary in opening factor, fire load, and size of the wood sticks.

All six columns failed during the compartment fire tests, with failure times ranging from 35 to 71 min [24]. In four of the tests, failure occurred during the decay phase of the fire. For one test, collapse occurred despite compartment temperatures remaining well below those of the ISO standard fire curve for most of the test. Thermocouple data again showed that temperatures in the section continue to rise through heat conduction throughout the cooling phase (i.e., thermal wave effect). This thermal wave, combined with the fact that the strength and modulus of timber experience severe reduction at temperatures as low as 100°C, progressively cause a major reduction in load-carrying capacity.

These experiments show the need for enhanced design measures, beyond standard fire resistance criteria, to mitigate the thermal wave effect and achieve stability until full burnout in natural fires. Therefore, the results from the compartment fire tests are used to calibrate a numerical model which is then employed to investigate the performance of columns with increased cross-sectional dimensions and to inform the new full-scale fire experiments.

3. Numerical analysis

3.1. Description of the finite element model

3.1.1. Thermal-structural modeling strategy

The response of the timber columns is analyzed using the nonlinear finite element software SAFIR® [29]. For each test, a thermal analysis is first conducted to evaluate the evolution of temperatures in the section of the column during the test. The temperature measurements from plate thermometers are used as the boundary in the model. Then, a mechanical analysis is performed to assess the structural response of the timber

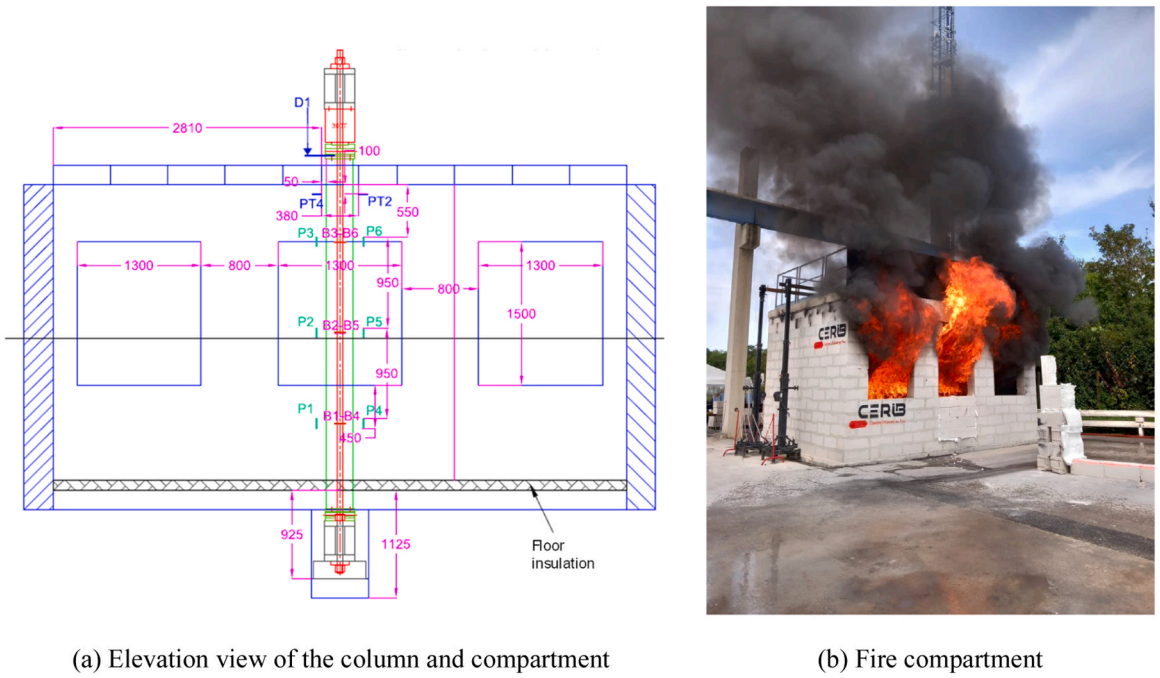

Fig. 1. Illustration of the compartment fire tests.

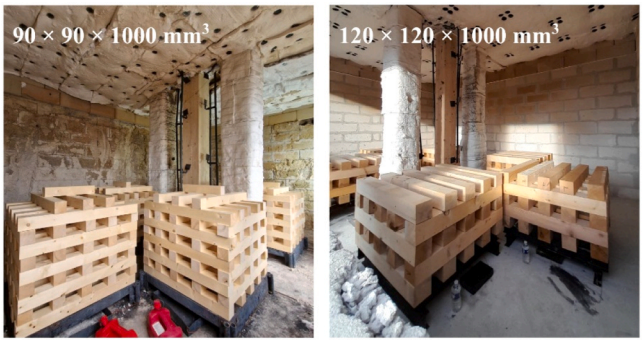

Fig. 2. Different configurations of wood cribs used in the compartment fire tests.

column under the applied load and varying internal temperatures. The section is discretized in fibers, and the analysis considers the reduction of strength and modulus in each fiber given its temperature at each time step of the analysis. The analysis is a geometrically and materially nonlinear analysis with imperfections included (GMNIA) that is run until either the column fails or the temperatures in the entire section have decreased back to ambient. The modeling strategy has previously been validated on a dataset of 49 standard fire tests on glulam columns [5]. More details on the thermal and mechanical models are provided below.

3.1.2. *Thermal model and properties*

The thermal analysis of the section of the column uses two-dimensional conductive solid elements. The heat transfer calculation considers conduction in the solid wood section, with convective and radiative heat transfer at the boundaries considering the effective fire temperature from the plate thermometers.

Temperature-dependent thermal properties are considered, adopting the effective relationships for the variation of thermal conductivity, specific heat, and density with temperature from Annex B of EN1995–1–2 [30]. In the thermal analysis, the geometry of the section is assumed to remain constant. The effective properties implicitly account for the mass transport effects, cracking, and charring in heated timber, from calibration on data obtained under standard fire exposure. As thermal exposure and environment influence the underlying processes implicitly captured by these properties, these effective properties of EN1995–1–2 may not be accurate under natural fire exposure with cooling phase; however, there is no established alternative model for the temperature-dependent relationships for timber applicable to natural fires. The objective here is to use the available models to extrapolate the response of new natural fire experiments, to design the test program. The specific mass of the timber is 480 kg/m^3, with a water content of 11 % of the dry mass, based on measurements on a timber column specimen at ambient temperature. The coefficient of convection is 35 W/(m^{2}K) and the emissivity is 0.8, and assumed constant, in accordance with Eurocode. The effect of temperature on the thermal properties is considered irreversible in the model.

3.1.3. *Structural model and properties*

The mechanical analysis of the timber columns is conducted using Bernoulli beam elements. The section of the beam element is discretized in fibers which are used for the heat transfer analysis (as the conductive solid elements) and for the mechanical analysis (as the fibers used for sectional integration). Integration on the section is performed, based on a fiber model, at two Gauss points along the length of each beam finite element. Each fiber in the beam section has its own area, mechanical properties, and temperature, resulting in its own stress-strain constitutive law at that temperature.

The stress-strain model is linear elastic-brittle in tension and linear elastic-plastic in compression. The input parameters include the elastic modulus E, the tensile strength f_t, the compressive strength f_c, and the limit strain for the plastic plateau in compression ε_{cu}. The limit strain in compression is set to $\varepsilon_{cu} = 0.02$ based on a recent numerical study [31]. At ambient temperature, the modulus is 11 500 MPa, while the nominal tensile and compressive strength are 27.6 MPa [26]. Like for thermal properties, the evolution of the mechanical properties with temperature is taken from Annex B of Eurocode EN1995–1–2. At each time step, the local values of the mechanical properties in each fiber are multiplied by the temperature-dependent reduction factor at the corresponding fiber temperature. Therefore, fibers with temperatures exceeding 300°C have

their modulus and strength drop to zero. The limit strain ε_{cu} is assumed to be constant with temperature. The effect of temperature on the mechanical properties is considered irreversible. Accordingly, at each time step, the strength and elastic modulus in a fiber are based on the maximum temperature that fiber has reached since the start of the fire. In other words, when a part of the timber section cools down, it does not recover its strength or stiffness, as the processes responsible for the degradation (such as dehydration and pyrolysis) are irreversible. Buckling is captured as the model accounts for large displacements and geometrical nonlinearities. An initial imperfection is introduced in the model to account for accidental eccentricities and out-of-straightness by considering a single sine curve with a mid-height maximum transversal deflection of L/400 (in accordance with Eurocode [32]) in addition to the 20 mm eccentricity of the load.

3.2. Analysis of the previous experiments

3.2.1. Temperatures in the columns

Temperatures inside the columns were measured during the tests along the centerline at various depths with 10 mm increments (i.e., at 10 mm depth, 20 mm depth, etc.), with 6 thermocouples (2 in the lower part of the column, 2 at mid-height, and 2 in the upper part) for each depth. Fig. 3 plots the average temperature at each depth as solid lines, while the range of temperature captured by each thermocouple is represented by a shaded area. The calculated temperatures from SAFIR are plotted as dashed lines. In the important temperature range of 100 °C to 300 °C, the model tends to overestimate the temperatures in the column section for Tests 9, 10, and 11, while it underestimates them for Test 14, 15, and 17. The discrepancy in temperatures between the model and the measurement varies from test to test, and within a test it varies at different depths. This variability underscores the uncertainties associated with predicting the thermal response of specific timber members (mainly because of the inherent inhomogeneity and variability of the

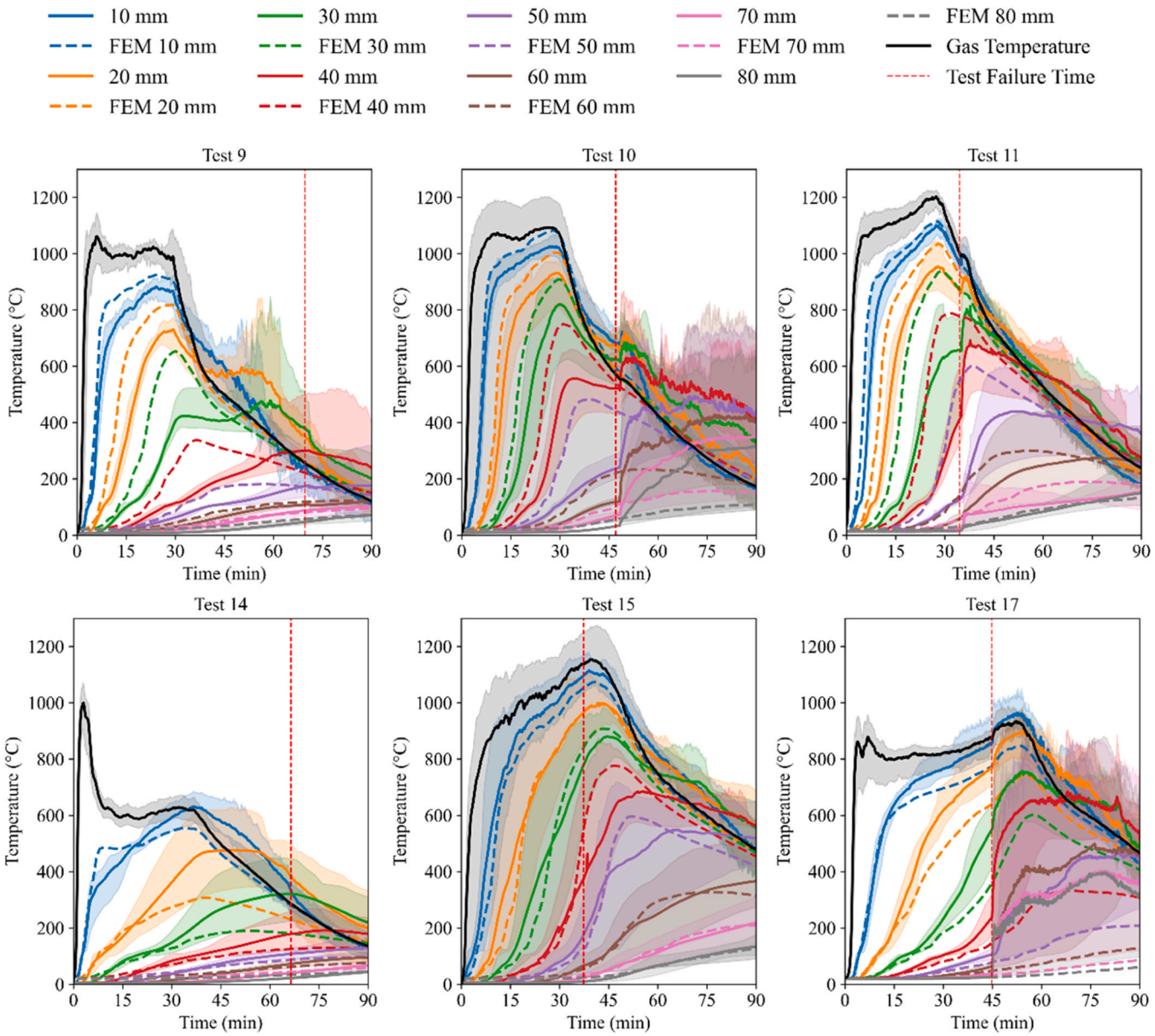

Fig. 3. Comparison of measured and computed temperatures in the cross-section of the timber columns, with thermal properties from Eurocode 5 and nominal parameters.

material, as shown by the extent of the shaded zones around each average curve). This highlights the need for further research on this aspect. Still, the model provides useful predictions of temperatures at any point in the section throughout the heating and cooling phases of the fire, using a given set of temperature-dependent thermal properties and parameters, for the purpose of informing the next experiments. The results from the thermal analysis are next used in the structural analysis.

3.2.2. Structural response

The structural analysis evaluates the response of the timber columns under applied load and the temperature increase calculated in the thermal analysis. The structural response of the columns in the six compartment fire tests was modeled using the temperatures from the thermal analysis. In all cases, the timber column failed. This outcome aligns with the experiments, which also resulted in failure for the six specimens. The failure times obtained in the experiment and calculated by the structural model are plotted in Fig. 4.

In addition to the failure times, it is useful to compare the profiles of maximum reached temperature in the sections at the time of failure. Fig. 5 plots these profiles from the model versus the experimental measurements. For test measurements, Fig. 5 is plotting the maximum values (over time) of the average curves (i.e., the solid curves in Fig. 3). The comparisons provide insights into the thermal conditions that led to failure for each column. This reveals that the sources of discrepancy in failure time between the model and the test (seen in Fig. 4) lie both in the thermal and mechanical models. For the thermal part, discrepancies in the transient fields of temperatures predicted by the model compared with the measurements have been shown previously (Fig. 3). Improving predictions of the kinetics of the thermal response will allow improving predictions of the time of failure. But at the same time, the comparison of temperature profile at failure shown in Fig. 5 also exhibits some discrepancy between the test and the model, particularly in the critical range of temperatures below 300 °C. The nonlinear temperature field that causes failure is not identical in the test and in the model. This suggests that, even if the thermal response was perfectly predicted, the mechanical model still would need to be further improved to improve prediction of the temperatures at which failure occurs. The simulated temperatures at the time of failure tend to be cooler than the corresponding experimental data, particularly deep in the section. This implies that the structural model is conservative, because it predicts failure of the column under a temperature profile not quite as severe as the temperature profile that triggered failure in the experiment. This could be due to the use of the strength reduction factors from Annex B of EN1995–1–2, which provide values generally lower than the average elevated-temperature strength data reported in the literature [33]. A previous numerical study on standard furnace tests has shown that the finite element models using these Annex B reduction factors tended to underestimate the fire resistance of the timber columns [5]. As a result, the thermal-structural finite element model is expected to provide conservative estimates of the response of the timber columns in the natural fire experiments. Overall, while areas for improvements have been identified and will be pursued in future works, the accuracy of the model was deemed sufficient to provide useful predictions of the thermal-structural response of timber columns with different cross-sections to support the design of the new experiments.

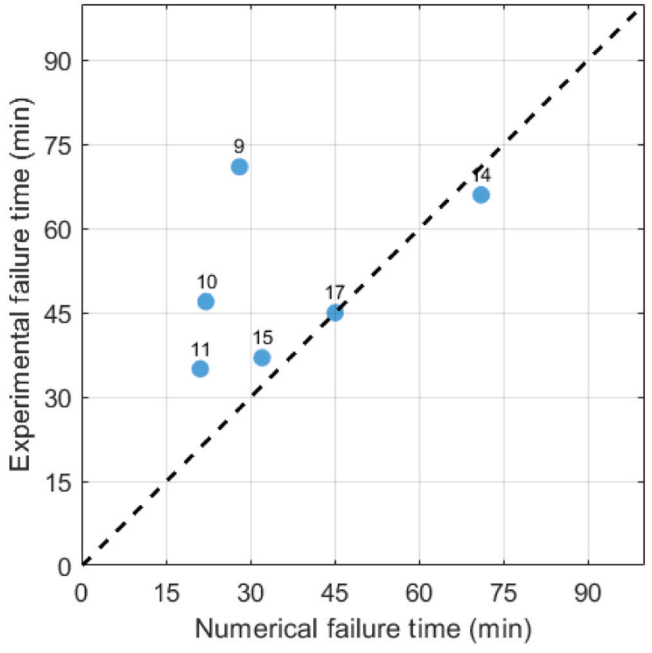

Fig. 4. Comparison of measured and simulated failure time for the six compartment fire tests on timber columns reported in [24]. The labels indicate the test number (Table 2).

3.3. Sizing the column sections for additional experiments

A parametric study is then conducted with the numerical model to assess the thermal-structural response of a new set of timber column specimens in the compartment fire. The objective is to mitigate the penetration of the thermal wave in the column section, that led to failure of all the specimens in the previous experiments (see Section 2). The strategy primarily focuses on increasing the size of the cross-section to allow part of the core to continuously remain at temperatures lower than 50–100 °C, thereby maintaining sufficient load-bearing capacity to survive the fire until burnout.

The fire exposure used in the parametric numerical analysis is the one from Test 10, which was produced with an opening factor of 0.065 $m^{1/2}$ and a fire load of 780 MJ/m^2. Test 10 is selected because this is the reference test in the compartment fire test program, as discussed in Section 4. Columns with cross-section sizes ranging from 300 × 300 mm^2 to 420 × 420 mm^2 with a step of 20 mm are studied numerically using the thermal-structural analysis approach described in Section 3. Importantly, the load on the column is kept the same (322 kN), as the objective is to increase the timber column section to achieve burnout resistance. The calculated design load-carrying capacity of the column with cross-section size of 280 × 280 mm^2 is 800 kN (using equations for a column subjected to combined compression and bending [32] with strength values of GL 24 h, as detailed in [22]). This leads to an utilization ratio (defined as the ratio of the applied load in the fire situation to the design capacity at ambient temperature) of 40 % for the 280 × 280 mm^2 column. This utilization ratio is gradually reduced as the timber column cross-section is increased, since the applied load is kept constant.

The results are summarized in Table 1. As expected, the fire performance of the column increases with an increase in its cross-section size (at constant load). However, to survive the fire until burnout, a significant size increase is required. It is worth noting that changing the section from 280 × 280 mm^2 to 400 × 400 mm^2 doubles the cross-section area and reduces the utilization ratio in the fire situation from 40 % to 17 %. The smallest section that achieves resistance to full burnout is the 380 × 380 mm^2 column. An inspection of the temperatures in the section confirms that this size increase mitigates the effect of the thermal wave, which allows the larger sections to maintain sufficient load-bearing capacity throughout the duration of the fire and decay phase. These numerical results were used to define the test program described in the next section.

4. Experimental program

Based on the numerical results, the minimum cross-section size for the column to attain sufficient load-bearing capacity throughout the natural fire is 380 × 380 mm^2. For the new compartment fire tests, it

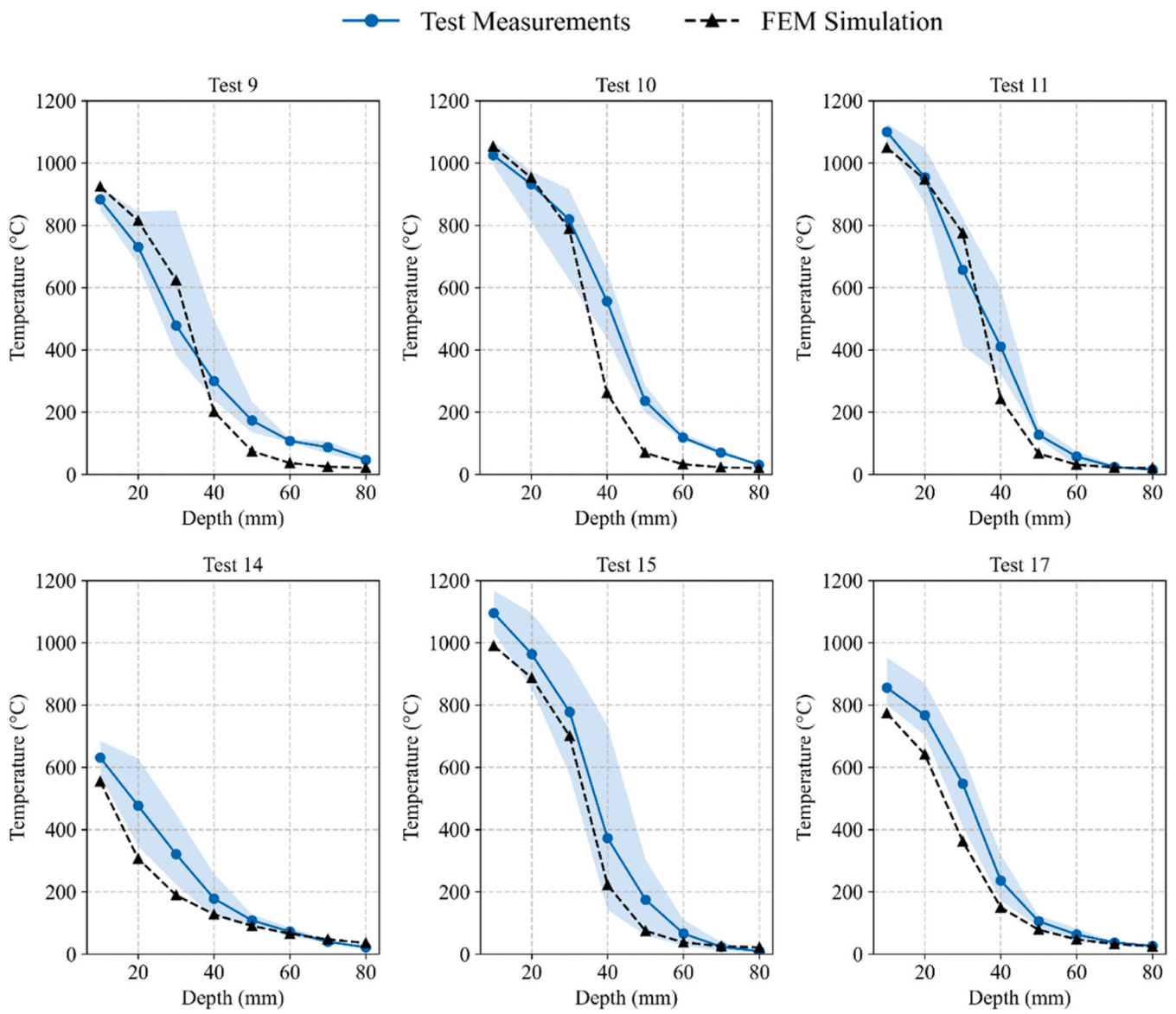

Fig. 5. Maximum section temperature at failure.

Table 1
Response evaluated by SAFIR for different timber columns exposed to the Test 10 fire until burnout.

Section Size (mm^2)	Failure Time Predicted by Model (min)
300 × 300	29
320 × 320	42
340 × 340	72
360 × 360	184
380 × 380	no failure
400 × 400	no failure
420 × 420	no failure

was decided to test columns with sections ranging from 340 × 340 mm^2 to 400 × 400 mm^2. These designs spanned across a range of expected behavior, where the 340 × 340 mm^2 was expected to still fail due to the thermal wave effect late in the decay phase, while the 400 × 400 mm^2 was expected to be large enough to withstand this effect. Besides the effect of section size, an additional test was conducted on a 280 × 280 mm^2 column but with water extinction 35 min after ignition. The time of intervention (35 min) was selected to ensure extinction before the expected failure time of the column and hence to allow observing the effect on the stability.

The test program is summarized in Fig. 6. Test 10, described in a previous publication [24], serves as reference test for the program. Test 10 was conducted on a glulam column with a section of 280 × 280 mm^2, used a fire load q = 780 MJ/m^2, opening factor O = 0.065 $m^{1/2}$, and wood cribs made of 10 layers of 5 sticks of 90 × 90 × 1000 mm^3 with 138 mm of clear distance between adjacent sticks. Test 12 is conducted on a column with section 340 × 340 mm^2. Test 13 uses a section of 360 × 360 mm^2. Tests 18, 19, and 20 use a section of 400 × 400 mm^2. Other than the section size, the test conditions used in Tests 12, 13, 18, and 19 are identical to those of the reference Test 10 [24]. Test 20 uses the same parameters except it uses an alternative wood sticks arrangement to maintain the fire load of 780 MJ/m2 but modify the burning rate, i.e., wood cribs made of 5 layers of 5 sticks of 120 × 120 × 1 000 mm^3 spaced by 100 mm and an amount of heptane reduced to 3 liters. Test 19 is a replicate of Test 18 but on a specimen that did not contain any thermocouple inside the section. This was to eliminate the possible influence of the groove, thermocouple wires, and defect in the gluing plane of the two halves of the column required for installation of thermocouples. Finally, Test 21 focuses on the effect of water extinction. It uses a 280 × 280 mm^2 section, which is the same as in the previous

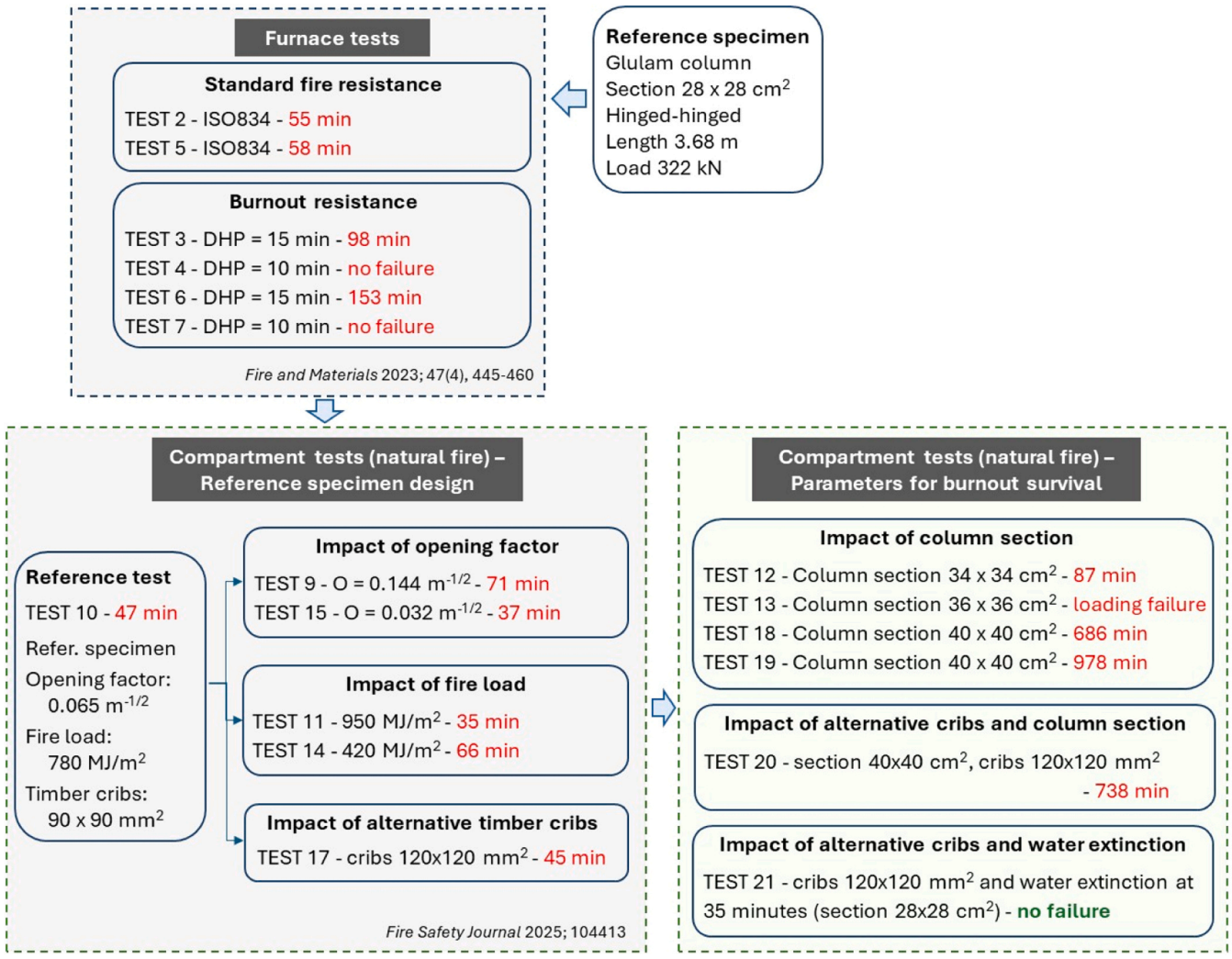

Fig. 6. Complete test program on glulam columns in fire (including data previously reported in [22,24]). The new tests, shown on the right, focus on columns with increased section or active suppression to investigate survival to burnout of natural fires.

experiments reported in Section 2.3. However, the fire is suppressed using water 35 min after ignition. Test 21 uses the alternative wood crib, like Test 20.

All tests are conducted on a glulam column subjected to the same load of 322 kN with an eccentricity of 20 mm in one direction. Note that the load is kept at the same value evaluated for the 280 × 280 mm^2 column in a representative five-story building even when testing the columns with larger section size, which results in a variation of utilization factor of the columns between the tests. Indeed, the objective here is to investigate the effect of increasing the timber column section at constant load to achieve burnout resistance. The load is applied prior to fire exposure and is held constant throughout the entire test, including the cooling phase.

The compartment dimensions are as given in Section 2.3 and shown in Fig. 1. The opening factor of O = 0.065 m$^{1/2}$ was obtained by having three openings of dimensions 1.30 × 1.50 m^2 in one of the long walls. The walls were made of 300 mm thick aerated concrete blocks. The concrete floor was insulated with mineral fiber and covered by a 20 mm layer of plasterboard. The roof consisted of 200-mm thick aerated concrete slabs.

For instrumentation, twelve plate thermometers (PT) were used to measure temperatures in the compartment. The PTs were positioned vertically facing outward on each side of the column, along the height of the column at three elevations, and with a distance from the column of 10 ± 5 cm, as shown in Fig. 7. Temperatures inside the columns were measured with 1.5 mm thick type K Inconel sheathed thermocouples along the centerline at various depths with 10 mm increments. For each depth, six thermocouples were used to measure temperature at three positions along the height of the column. The thermocouples were installed parallel to the expected isotherms. The inner wires circulate through milled grooves and exit at the bottom of the column. The influence of these millings was investigated in [22], and the results showed that the milling grooves had no significant influence on the load-bearing behavior. The gas analyzer probe opening was placed near the rear wall, at 2.88 m height, at around 1.2 m from the right-hand side wall. Heat flux data was recorded by two heat flux meters placed at 3 m and 8 m from the opening. More details on the compartment and fire test methodology are provided in a previous study [24].

5. Experimental results

5.1. Main outcomes and failure time

The experiments were conducted in 2022 and 2023 at the Fire Testing Centre of CERIB in France. The main parameters and outcomes are summarized in Table 2. Collapse time was determined as the time at which the column lost ability to withstand the target load, as indicated by a drop in the value of the force that the hydraulic system could apply.

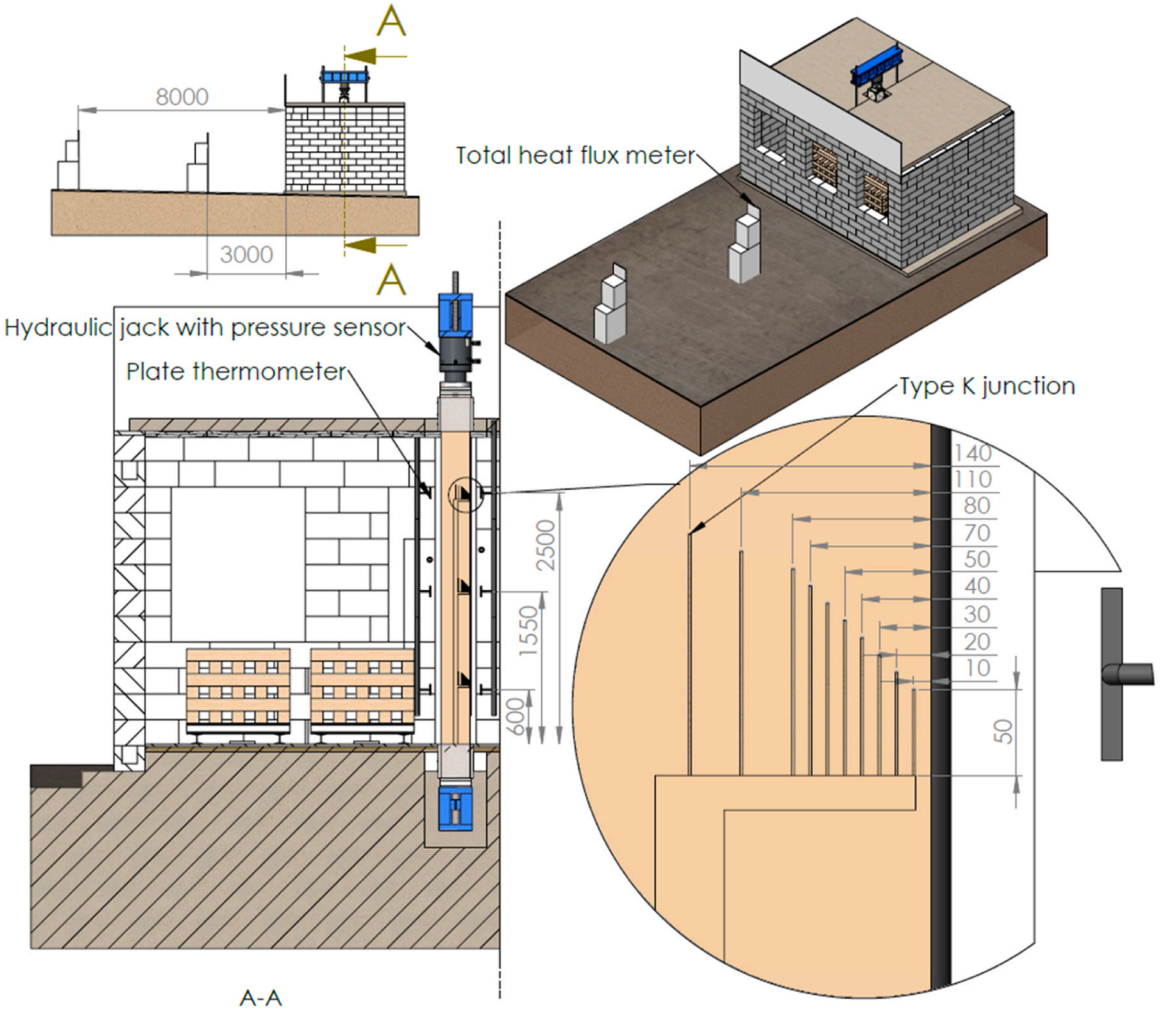

Fig. 7. Glulam column in the compartment with its instrumentation.

Table 2
Summary of results from the twelve compartment fire tests on glulam columns.

Test	A (mm^2)	O ($m^{1/2}$)	q (MJ/m^2)	wood crib (mm^2)	T_{max} (°C)	End heating phase (min.)	Collapse (min.)
9	280 × 280	0.140	780	90 × 90	1000	30	71
10	280 × 280	0.065	780	90 × 90	1150	30	47
11	280 × 280	0.065	950	90 × 90	1200	28	35
14	280 × 280	0.065	420	90 × 90	600**	36	66
15	280 × 280	0.032	780	90 × 90	1250	40	37
17	280 × 280	0.065	780	120 × 120	915	55	45
12	340 × 340	0.065	780	90 × 90	1150	28	87
13	360 × 360	0.065	780	90 × 90	1180	30	> 98*
18	400 × 400	0.065	780	90 × 90	1200	31	686
19	400 × 400	0.065	780	90 × 90	1170	27	978
20	400 × 400	0.065	780	120 × 120	850	45	738
21	280 × 280	0.065	780	120 × 120	900	35** (suppression)	no failure

* instability of the loading system.
** firefighter intervention.

The first six experiments, conducted on identical columns made of 280 × 280 mm^2 glued laminated timber section and reported in a previous publication [24], are included in the first six rows of the table. These six experiments all failed under the compartment fire, with two failures during the heating phase and four failures during the cooling phase.

The six new experiments are reported in the bottom part of the table. In Test 12, the column failed after 87 min, during the decay phase. For Test 13, localized continuous burning, due to the presence of an air gap at the top of the column, provoked an instability of the loading system at 98 min, so the test was inconclusive. In Tests 18, 19, and 20, conducted on the columns with 400 × 400 mm^2 section, failure occurred late in the decay phase, 11–16 h after ignition. Therefore, in the absence of fire suppression, the timber columns failed to survive the fire to full burnout. Pictures of the experiments are provided in Fig. 8.

Detailed analyses of the tests, provided hereafter, show that failure

Fig. 8. Pictures of three of the compartment fire tests on glulam columns.

was primarily due to continued strength reduction with thermal wave penetration during the decay phase for the smaller section (Tests 12), and due to localized smoldering for the larger sections (Tests 18, 19, 20). The only column that survived until burnout was the one with the original 280 × 280 mm^2 section but with active fire suppression after 35 min.

5.2. Temperatures in the compartment

During the tests, the temperatures in the compartment were collected through 12–16 plate thermocouples (PT). The average temperatures in the compartment are plotted in Fig. 9. The curves are interrupted with a dot at the time of failure of the column. For Test 21, no failure of the column was observed owing to the fire extinction by water at 35 min.

Tests 12, 13, 18 and 19 had nominally identical conditions for the fire in the compartment, differing only by the size of the column section. The evolution of average exposure temperature was similar across these tests. The temperatures exceeded 1000 °C in 3–6 min, then reached a peak in the 1150–1200 °C range within 27–31 min, followed by a cooling at an average rate of about 20 °C/min over the next 20 min. Tests 20 and 21, with larger sticks in the wood crib, exhibited a slower temperature rise and a lower peak, in the 850–900 °C range.

The evolution of oxygen concentration within the compartment is

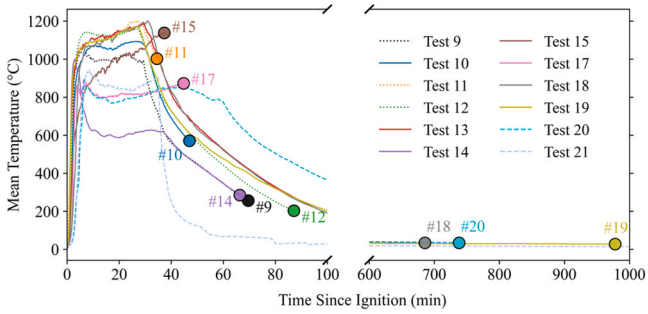

Fig. 9. Evolution of the average temperature in the compartment during the natural fire tests. Failure of the timber columns is marked by a dot on the curves.

shown in Fig. 10, while the heat flux data, recorded by two heat flux meters placed at 3 m and 8 m from the opening, are presented in Fig. 11. Again, a distinction is visible between the tests using the smaller sticks (Tests 12, 13, 18 and 19) and the ones with the larger sticks (Tests 20 and 21). The former were more intense and more clearly ventilation-controlled during the heating phase likely due to the larger fuel area exposed. This is evident from the sharp drop in oxygen concentration shortly after ignition, with values falling close to 0 % within the first 10 min. During this period, heat flux readings, particularly from Heat Flux Meter 1 (located 3 m from the opening), peak at approximately 20–30 kW/m^2, indicating intense flaming combustion near the compartment opening. Meter 2, located farther from the compartment opening (at 8 m vs. 3 m), consistently records lower values, around 10 kW/m^2. The oxygen concentration begins to recover around the 30–40 min mark, gradually rising back to 21 % as the fire decays. The heat flux data show a rapid rise within the first 5 min, a sustained peak between 5 – 35 min, and a gradual decline after 35 min, consistent with a fully developed fire followed by decay. Note that the oxygen reading for Test 13 was deficient. For Tests 20 and 21, in contrast, the use of larger wood sticks resulted in a less intense fire, with a heat flux peaking at 10–15 kW/m^2.

5.3. Temperatures and charring in the columns

The temperatures inside the timber columns are measured at different depths in the section. For each depth, there are either five or six measurements along the column at that depth. The results are plotted in Fig. 12, where black lines refer to the compartment temperature, solid lines represent the average temperature at each depth, and the shaded areas indicate the range of the temperatures measured at that depth. As expected in natural compartment fires, the compartment temperature displays some spatial variability as shown by the width of the black shaded area; however, this variability remains generally limited to about 100 °C.

The plots clearly illustrate the thermal wave effect: while peripheral parts of the section heat up fast and then cool down with the compartment temperature, the temperature at the center of the cross-section keeps rising for more than one hour after the time of peak temperature in the compartment. In Test 21, however, the water suppression of the fire and associated spraying of the timber column alongside the removal of the char layer is effective at dramatically reducing the thermal wave. The temperature rise in the central part of the section is shorter and of lower magnitude than for the fire tests with no suppression.

In this study, the charring is indirectly determined from the measured temperatures in the timber column. Defining charring based on the threshold of 300°C as assumed according to EN 1995–1–2, the average charring rate is evaluated for a zone between two thermocouples from the time at which each thermocouple at different depths from the exposed surface reached this temperature. The detailed results of the

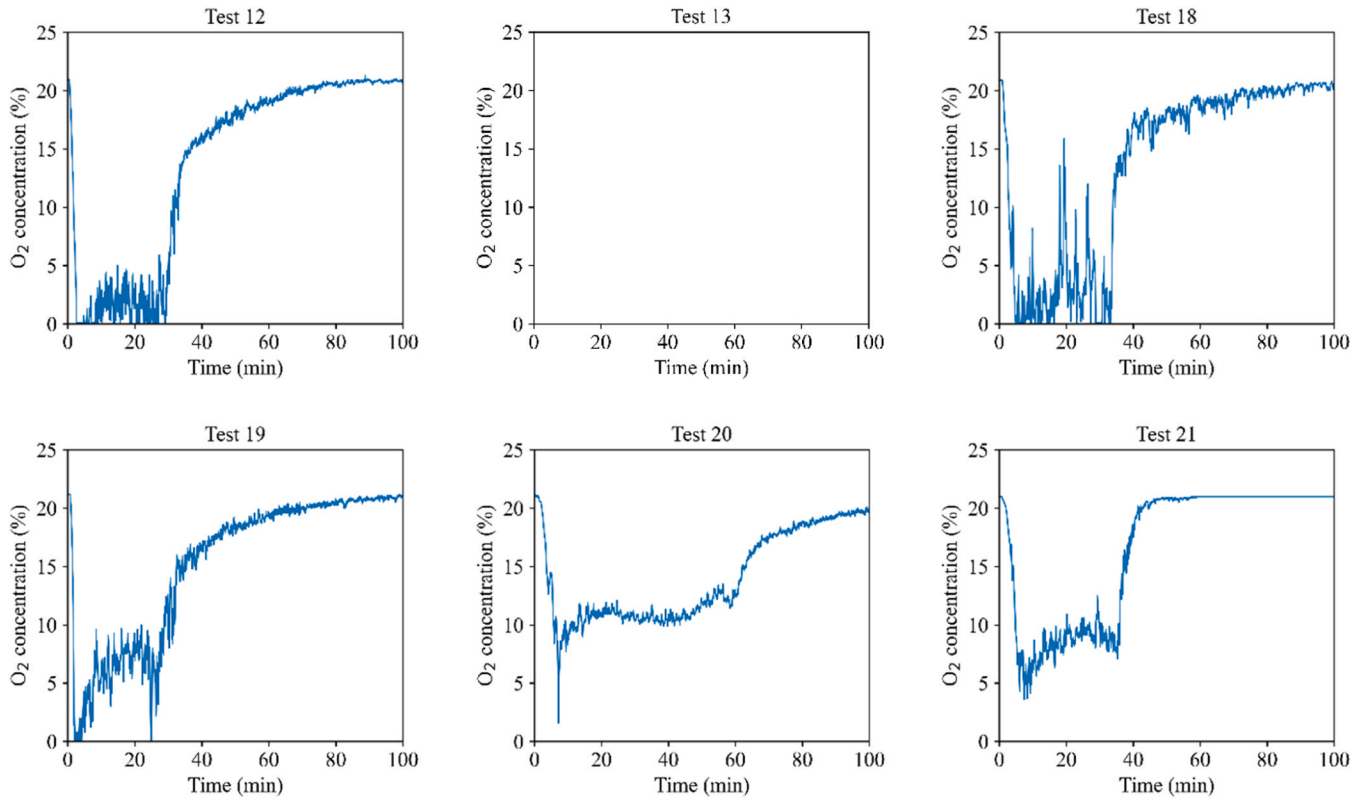

Fig. 10. Variation of oxygen concentration in the compartment during the tests.

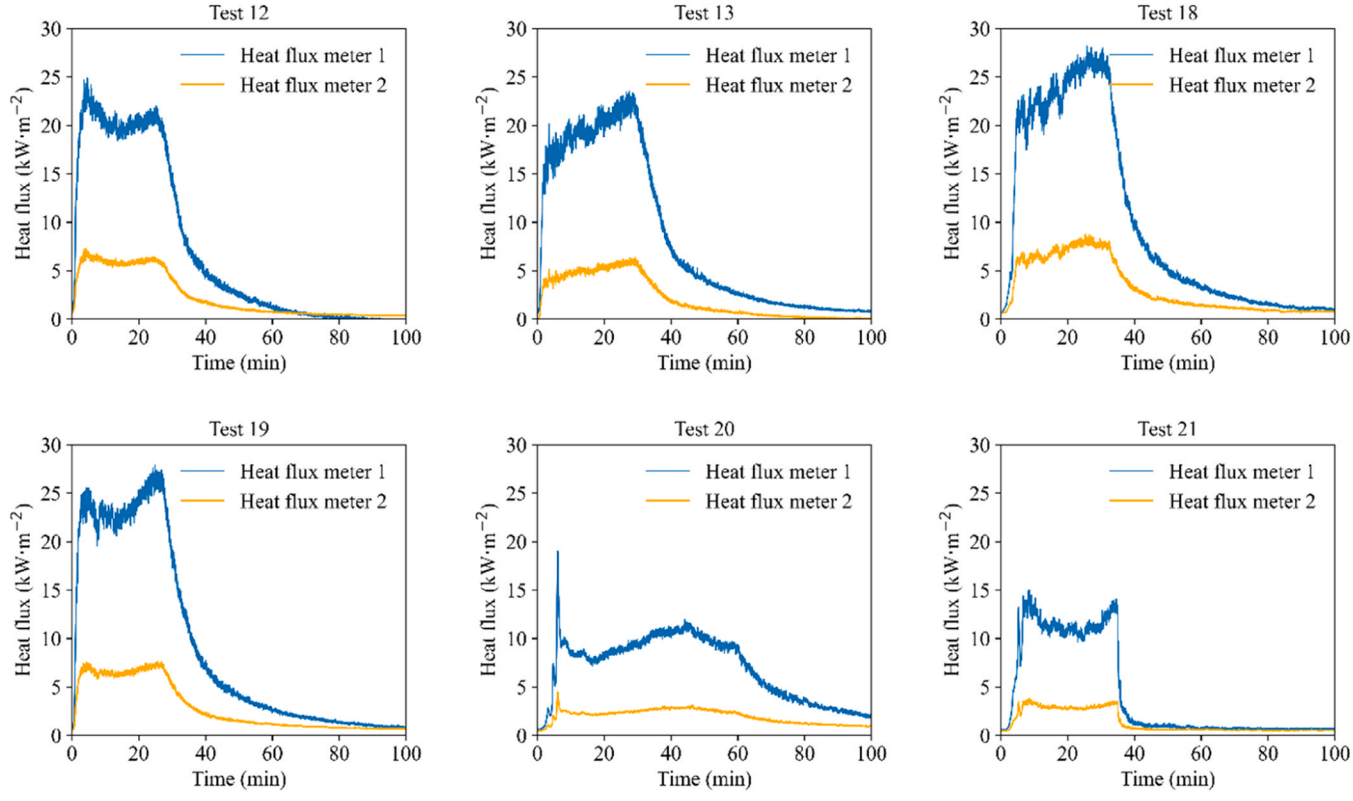

Fig. 11. Variation of heat flux in the compartment during the tests. (heat flux meters 1 and 2 are located at 3 m and at 8 m from the opening, respectively).

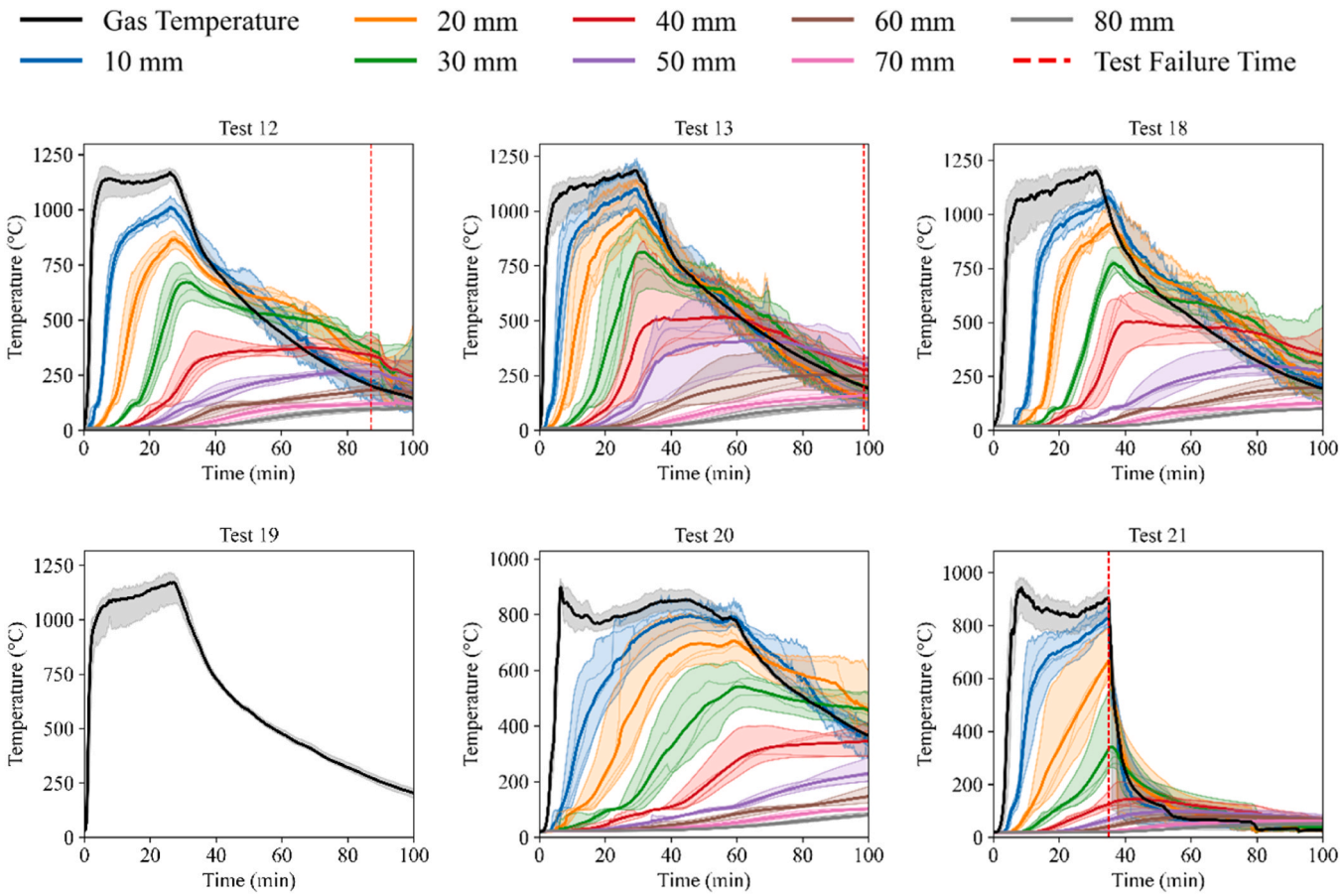

Fig. 12. Distribution of the temperature within the column section. (Note: Test 19 did not contain thermocouples in the section. Test 21 was subject to water extinction at 35 min).

Table 3
Average charring rate (mm/min) for different zones along the depth.

	0–10 mm	10–20 mm	20–30 mm	30–40 mm
Test 12	1.74	1.69	1.05	0.78
Test 13	2.00	2.14	1.05	1.29
Test 18	0.89	1.76	1.11	1.38
Test 20	0.91	0.82	0.68	0.39
Test 21	1.42	1.04	0.66	-

(*) the specimen of Test 19 did not contain any thermocouples in the section.

charring rate for different tests are listed in Table 3.

6. Discussion

6.1. Thermal wave effect

The effect of the thermal wave can be observed from the thermocouple measurements in Fig. 12. This effect is primarily responsible for the failure during the decay phase of the fire of Test 12 on the 340 × 340 mm^2 section. It was also identified as the cause of failure for

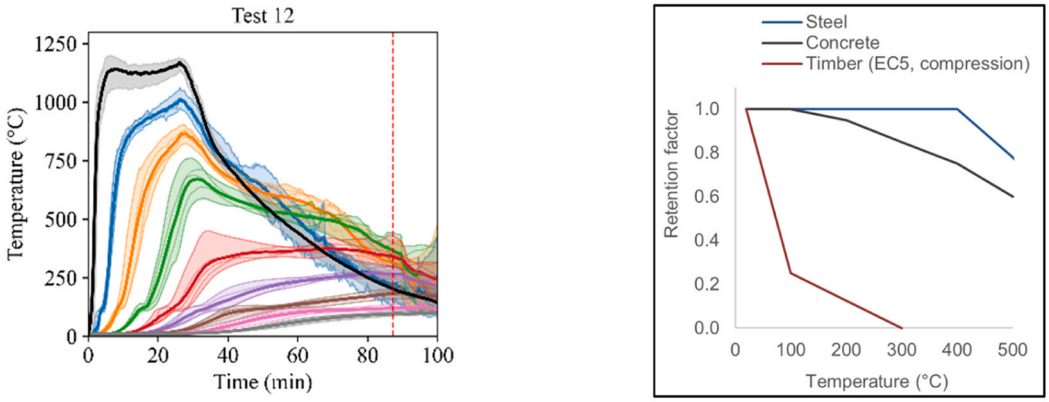

(a) Thermal wave in the section of a timber column (b) Reduction in strength with temperature

Fig. 13. The thermal wave effect: combination of delayed heating in the section core and severe reduction of properties with moderate temperature in timber.

the previous series of tests on the 280 × 280 mm^2 section in the furnace [22] and in the compartment tests [24]. In Test 12, the thermocouple measurements indicate that although the outer perimeter of the section has begun to cool, temperatures at a depth larger than 50 mm were still rising when the column failed at 87 min. This delayed thermal penetration led to continued degradation of the load-bearing capacity of the column, due to the severe effect of temperature on the strength (Fig. 13) and stiffness of timber, ultimately causing structural failure during the cooling phase. The numerical model had correctly predicted that the 340 × 340 mm^2 section would fail during the cooling phase, based on modeling that captures the heat transfer process in the section and its effect on the structural response.

Tests 13, 18, 19, and 20 involved timber columns with increasingly large sections. The 360 × 360 mm^2 section of Test 13 maintained stability for 98 min, at which point a malfunction of the loading system led to the interruption of the test. No conclusion is therefore drawn from this test, other than the fact that the column survived at least for 98 min. The next three tests (18, 19, and 20) were performed on 400 × 400 mm^2 section. The columns failed in each of these tests. In Test 18, failure occurred 11 h 28 min after the start of the test, at a time when the compartment temperature had dropped to 34 °C. Test 19, conducted under the same fire and loading conditions as Test 18, but with no internal thermocouples, collapsed after 16 h 18 min, at a time when the compartment temperature was only 28 °C. Finally, Test 20, which used different wood cribs, failed after 12 h 18 min. So late in the experiment, the temperatures had had the time to rise, peak and decrease, even at the center of the cross-section, as verified by the thermocouple measurements. Therefore, the thermal wave effect was not the primary cause of failure for the 400 × 400 mm^2 section. The numerical model predicted that the columns with 400 × 400 mm^2 section would survive the fire until burnout, yet they failed, but much later than the smaller sections and not due to the continued rise in internal temperatures. Instead, inspection of the data and observations from the experiments revealed that localized smoldering had taken place in these experiments, slowly weakening the columns, until eventual failure. Smoldering is a mechanism distinct from the thermal wave, unfolding over a longer time, and which can also result in failure during the cooling phase, as discussed hereafter.

6.2. Role of smoldering

Analysis of Tests 18, 19, and 20 conducted on the larger 400 × 400 mm^2 section revealed the role of smoldering in late failure of the columns. In Test 18, a construction defect was found before the test, in the form of a longitudinal gap between the two halves of the column, reaching up to 35 mm deep in some spots. This gap was filled with an intumescent material over a length of 69 cm on one side and 197 cm on the other. However, this local intervention was not sufficient to prevent local glowing during the test. After the test, the two halves showed different levels of damage. This test illustrated that defects along gluing planes in GLT can weaken structural performance in fire. It also points to the importance of fast inspection and suppression in a fire event to avoid further damage from smoldering.

Although this was not the subject of this research work, the influence of the grooves raises questions about the influence of longitudinal shrinkage cracks which are often present in solid wood members in, for example, heritage buildings.

Test 19 was carried out in the same conditions as Test 18, but on a section without any thermocouples inside the column and with no visible defect. The column nevertheless collapsed 16 h and 18 min after the test began, when the compartment temperature was 28°C. After the test, it was clear that the bottom of the column had experienced much more severe charring and combustion than the rest of the section, see Fig. 14. Whereas around 0.080 m^2 of the initial section of 0.160 m^2 remained for most of the sections, there remained only 0.035 m^2 of it at the base of the column.

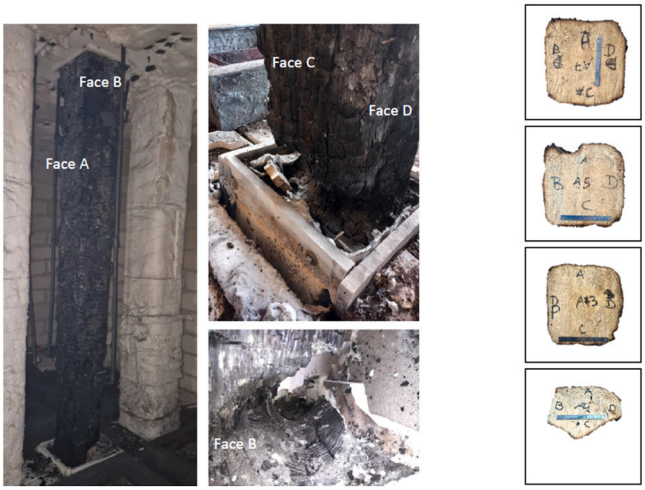

Fig. 14. Smoldering in Test 19.

After Test 19 revealed the damaging effect of severe charring at the base of the column, a closer look at the images from Test 18 suggested that a similar pattern may have occurred there as well, although the impact of the mid-height defect was more pronounced.

Test 20 exhibited a relatively similar behavior to Test 19. The column seemed to be surviving the whole fire duration when collapse occurred suddenly 12 h and 18 min after the beginning of the test, at a time when the compartment temperature was at 34°C with, again, a severe reduction of the section at the base of the columns.

The cause of the charring combustion near the base remains uncertain. One possibility is sustained radiation from the embers of the fire load resting on the floor, even if they are present only at the earlier stage of the charring. Another possible explanation may be the radiation emitted by the heated floor surface, although this would suggest a similar effect at the ceiling, which was not observed. A third possibility is the presence of a gravity-driven flow of fresh, oxygen-rich air along the floor, which could have intensified combustion at the base of the column.

Note that late failures of structural timber members due to continued smoldering have been reported recently by two other groups of researchers [6,34]. In the study by Wiesner et al., the collapse of a cross-laminated timber slab 29 h after the onset of heating was attributed to continued in-depth smoldering. In the latter study, an additional test with a larger opening led to survival of the structure.

6.3. Effect of firefighter intervention

Test 21 served to investigate the effect of firefighter intervention (water extinction), see Fig. 15. The tested column had a cross-section of 280 × 280 mm^2, and the firefighter intervention started 35 min after ignition. At this time, firefighters sprayed water in the compartment from the outside with a water hose to extinguish the wood cribs and reduce the temperatures in the compartment, then sprayed the column and finally entered in the compartment to scratch the charred layers away from the column. The amount of water used in the intervention was roughly 1 m^3. The column maintained its stability until the full cooling with no failure.

The heat flux and oxygen concentration data in Fig. 10 and Fig. 11 indicate that the intervention effectively interrupted the combustion process and initiated an early cooling phase. Further, the extensive water spraying dramatically reduced the thermal wave effect and prevented smoldering-related delayed failure. The temperatures inside the section at a depth of 10, 20 and even 30 mm from the surface decrease nearly immediately after the intervention. Still, it is noteworthy that the temperature rise at the center of the section, at a depth of 140 mm, still

Fig. 15. Extinction at 35 min in Test 21.

lasted for more than 4 h. This continued temperature rise occurred despite the removal of an approximately 30-mm thick layer of char, taking away with it the thermal energy that it contained, and reducing the distance from the central zones to cold air. Nevertheless, this continued heating of the inner part of the section had been reduced significantly by the intervention as seen in Fig. 12. These results highlight the critical role that firefighter intervention can play in preserving the integrity of timber structures. While the intervention successfully enabled the column to maintain stability to burnout, it is important to emphasize that timely and extensive water application to the timber framing members cannot be relied upon as the sole component of the fire safety strategy in situations where occupant life safety could be compromised (e.g., in tall buildings); structures should also have sufficient inherent capacity to withstand the fire.

6.4. Numerical model

The numerical analysis of the six previous compartment fire tests has shown that FE models are useful to capture the thermal and structural response of glulam columns exposed to natural fire and improve understanding of the phenomena influencing burnout resistance, but efforts are still required to improve accuracy, and smoldering is not captured.

Numerical simulations can be used to assess the relationship between the size of the cross-section, the thermal wave, and the resulting reduction in load-bearing capacity. The numerical model with SAFIR had correctly predicted the delayed failure of the 340 × 340 mm^2 section, based on modeling of the heat transfer in the section throughout the heating and cooling phase and its effect on the structural response. In contrast, the model had predicted that the 400 × 400 mm^2 section would survive the fire until burnout. While the latter in fact failed, failure was not due to the thermal wave effect but to smoldering that occurred more than 10 h after ignition. Smoldering is a phenomenon that is at this stage not present in numerical models. The model had correctly evaluated the increase in section size needed to mitigate the thermal wave effect and remain stable during the cooling phase, notwithstanding continued smoldering. The experiments thus suggest that numerical modeling can be used to design timber members for burnout resistance, provided localized smoldering is mitigated through other means, such as thorough inspection and suppression of hot spots after a fire

Enhancements in numerical models should focus on effective thermal properties that capture the effect of thermal exposure, in order to improve the accuracy of heat transfer models under natural fires that include a cooling phase. The temperature-dependent mechanical properties currently provided in Eurocode 5 should also be revisited, as pointed out by a recent study [33]. The experiments described in this paper highlight that smoldering should also be considered when focusing on stability of timber structures until burnout. It is likely that the smoldering issue will not be solved by modeling in the near term but rather has implications for active fire suppression and post-fire inspection. Encapsulation of the members, notwithstanding the positive effect that it will have on delaying the thermal wave, could in this respect raise a challenge as the protective layers should be taken away to allow inspection. In case of a large structure with many members involved in the fire, safely conducting such an inspection might be challenging.

Finally, the variability observed in experiments and the agreement between measurements and models highlights the complexity and uncertainty associated with the fire response of timber members; sensitivity analyses and calibration based on test data on specimens are therefore recommended to enhance confidence in the models.

6.5. Design for burnout resistance

These compartment fire experiments have highlighted two key failure modes during the decay phase for timber columns under natural fires, as shown in Fig. 16.

The first mode, referred to as ‘thermal wave’, is due to the continued heating of the interior part of the section from the periphery and charred layer, even as the external heat influx has ceased or has even turned negative. This continued heating leads to a delayed temperature rise in the center of the section, which leads to strength and stiffness reduction of the column, as illustrated in Fig. 13. This behavior has been evidenced through thermocouple data from furnace tests [22] and compartment fire tests [24], and the accompanying structural failure of the loaded columns, as well as through numerical modeling [5]. This study has shown that increasing the size of the cross-section of a timber column (at constant load) is an efficient strategy to mitigate this behavior. In the considered case, a major size increase was needed: the timber column designed for a five-story building as a 280 × 280 mm^2 section had to be increased to a 400 × 400 mm^2 section to survive the thermal wave effect until full burnout. In cases where the original section is already larger, it is expected that the required size increase may be more modest, as less heat from the natural fire would reach the center of the section. Such an approach is of course not without any consequence on the architectural aspect and on the usable floor surface area.

The second failure mechanism is related to smoldering. These experiments have shown that, left unattended, even the 400 × 400 mm^2 timber columns eventually failed more than 10 h after ignition. These failures occurred after the temperatures had peaked and started decreasing in the central zones of the section, indicating that the failure is not caused by the sole thermal wave effect. Instead, localized smoldering at the base or at defect locations (e.g., glue lines) led to gradual section loss and, eventually, structural failure, as shown in Fig. 17 for Tests 18, 19, and 20. These observations corroborate findings by others, such as collapse of a cross-laminated timber (CLT) slab 29 h after ignition [35], and failure of an unloaded column 32 h after the end of flaming due to extensive smoldering at the base of the column in the

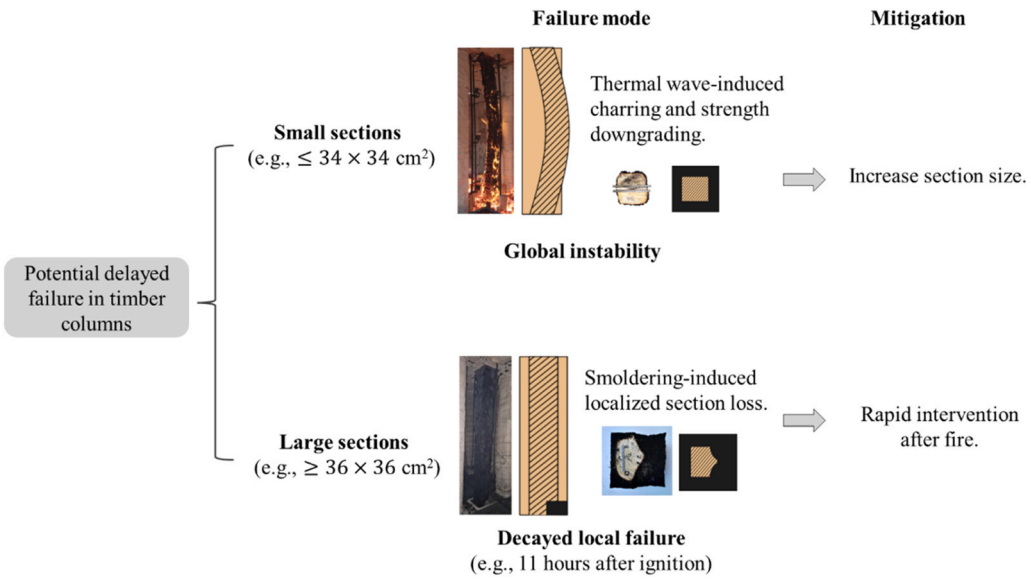

Fig. 16. Two failure mechanisms for timber columns during the decay phase of a natural fire. (Note: the indicated section sizes are applicable for the experiments considered but would vary for other conditions such as loading and fire parameters).

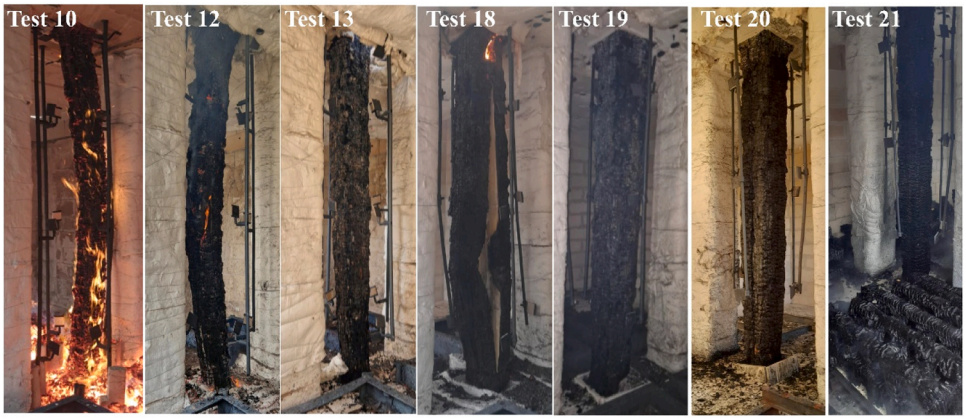

Fig. 17. Pictures of the timber columns at the end of the fire tests.

Code Red #2 experiment [36]. Smoldering poses serious safety concerns, also considering that it may develop unnoticed behind encapsulation [21]. While this is a complex mechanism that cannot be predicted by current models, active and extensive water suppression has been effective in the studied setup at stopping smoldering, as demonstrated by Test 21.

It is noteworthy that the timely active fire suppression used in Test 21 proved successful at mitigating both the thermal wave and smoldering sufficiently to achieve burnout resistance with the original section size of 280 × 280 mm^2. In design, when burnout resistance is the target objective, the two parameters of section size and active suppression should be considered jointly. In tall buildings, where access can be challenging and/or multiple columns might be involved in the fire, timely and extensive application of water on the timber members cannot be relied upon as the sole fire safety strategy. Based on our experiments, it seems generally recommendable to increase the section size to mitigate the thermal wave, while still requiring thorough inspection and intervention in the hours after the fire to suppress smoldering.

7. Conclusions

Previous tests on 3.7 m long, 280 × 280 mm^2 glulam columns designed for 60 min of fire resistance showed failure during compartment fires, often in the decay phase due to the continued heating of the core of the section. In this study, six new fire tests were carried out on larger columns (340 × 340 mm^2 to 400 × 400 mm^2) under identical mechanical load, fire load, and ventilation conditions. Increasing the cross-section to 400 × 400 mm^2 delayed failure beyond the time of peak temperatures inside the section, but smoldering ultimately led to collapse of the columns. The tests highlighted two distinct mechanisms of delayed failure during the decay phase: (1) thermal-wave-induced strength loss, observed in the smaller section (340 × 340 mm^2) column, where internal temperatures were still rising when collapse occurred; and (2) smoldering-driven degradation, observed in the larger section (400 × 400 mm^2) columns, which survived until the thermal wave had peaked in the section but then failed over 11 h after ignition due to smoldering, particularly near the column base.

In a subsequent test on a 280 × 280 mm^2 column, early firefighter intervention successfully prevented failure. The intervention, in which firefighters extinguished the fire after 35 min, cooled the section, and removed the char layer, prevented both thermal wave progression and smoldering. The column survived the full test without failure, underscoring the effectiveness of active suppression.

Numerical analyses by finite element modeling proved useful to investigate the thermal-structural response of the timber columns under natural fire and inform the design of the test program. Analyses were

conducted before the tests to select the cross-section sizes. The models can be used to evaluate the effect of column design on the thermal wave effect and stability until burnout. Yet, model accuracy is limited by the accuracy of the thermal and mechanical models and properties, which were calibrated for standard fire exposure; future works should focus on developing more advanced properties applicable for various thermal exposures. While prediction of smoldering appears out of the state of the art of structural fire resistance models, the implications for design and firefighter intervention should be carefully considered.

This work advances the understanding of the structural behavior of timber columns during the decay phase of natural fire, especially for axially loaded members designed to resist the thermal wave effect. The findings suggest that achieving burnout resistance in timber structures requires a combination of adequate thermal-structural strength with thorough inspection and water suppression during and after the fire, in particular to prevent continued smoldering that could result in failure several hours after the temperatures in the compartment have returned to ambient. Future works will aim to develop design methods for burnout resistance.

CRediT authorship contribution statement

Jochen Zehfuß: Writing – review & editing, Validation, Methodology. **Jean-Marc Franssen:** Writing – review & editing, Software, Methodology, Conceptualization. **Silvio Renard:** Writing – review & editing, Methodology, Investigation, Formal analysis, Data curation. **Chenzhi Ma:** Writing – original draft, Visualization, Software, Formal analysis. **Fabienne Robert:** Writing – review & editing, Resources, Project administration, Methodology, Funding acquisition, Conceptualization. **Patrick Bamonte:** Writing – review & editing, Validation, Methodology. **Robert McNamee:** Writing – review & editing, Validation, Methodology. **Thomas Gernay:** Writing – original draft, Validation, Software, Methodology, Investigation, Conceptualization.

Declaration of Competing Interest

The authors declare the following financial interests/personal relationships which may be considered as potential competing interests: Thomas Gernay reports financial support was provided by National Science Foundation. Fabienne Robert, Silvio Renard reports financial support was provided by France Assureurs. Under a license agreement with Gesval S.A., Dr. Gernay is entitled to royalty distributions related to technology SAFIR described in the study discussed in this publication. This arrangement has been reviewed and approved by the Johns Hopkins University in accordance with its conflict of interest policies. If there are other authors, they declare that they have no known competing financial interests or personal relationships that could have appeared to influence the work reported in this paper

Acknowledgements

The support from the French Federation of insurers FRANCE ASSUREURS is gratefully acknowledged. This material is partly based upon work supported by the U.S. National Science Foundation under award No. 2420368 (PI: T. Gernay).

Data Availability

Data will be made available on request.

References

[1] Ilgın HE, Karjalainen M, Pelsmakers S. Contemporary tall residential timber buildings: what are the main architectural and structural design considerations? IJBPA 2023;41:26–46. https://doi.org/10.1108/IJBPA-10-2021-0142.

[2] Churkina G, Organschi A, Reyer CPO, Ruff A, Vinke K, Liu Z, et al. Buildings as a global carbon sink. Nat Sustain 2020;3:269–76. https://doi.org/10.1038/s41893-019-0462-4.

[3] S. Kurzinski, P. Crovella, P. Kremer, Overview of Cross-Laminated Timber (CLT) and Timber Structure Standards Across the World, 5; 2022.

[4] A. Law, R. Hadden, We need to talk about timber: fire safety design in tall buildings, The Structural Engineer; 2020.

[5] Gernay T. Fire resistance and burnout resistance of timber columns. Fire Saf J 2021;122:103350. https://doi.org/10.1016/j.firesaf.2021.103350.

[6] Wiesner F, Bartlett A, Mohaine S, Robert F, McNamee R, Mindeguia J-C, et al. Structural capacity of one-way spanning large-scale cross-laminated timber slabs in standard and natural fires. Fire Technol 2021;57:291–311. https://doi.org/10.1007/s10694-020-01003-y.

[7] Gernay T. Performance-based design for structures in fire: advances, challenges, and perspectives. Fire Saf J 2024;142:104036. https://doi.org/10.1016/j.firesaf.2023.104036.

[8] Xu H, Pope I, Gupta V, Cadena J, Carrascal J, Lange D, et al. Large-scale compartment fires to develop a self-extinction design framework for mass timber—Part 1: literature review and methodology. Fire Saf J 2022;128:103523. https://doi.org/10.1016/j.firesaf.2022.103523.

[9] International Organization for Standardization (ISO), ISO 834-1: 2025, Fire-resistance tests — Elements of building construction — Part 1: General requirements; 2025.

[10] Schmid J, Klippel M, Just A, Frangi A. Review and analysis of fire resistance tests of timber members in bending, tension and compression with respect to the reduced cross-section method. Fire Saf J 2014;68:81–99. https://doi.org/10.1016/j.firesaf.2014.05.006.

[11] Lucherini A, Pitelková DŠ, Mozer V. Predicting the effective char depth in timber elements exposed to natural fires, including the cooling phase. In: Proceedings of the World Conference on Timber Engineering (WCTE 2023); 2023. https://doi.org/10.52202/069179-0226.

[12] Mitchell H, Kotsovinos P, Richter F, Thomson D, Barber D, Rein G. Review of fire experiments in mass timber compartments: current understanding, limitations, and research gaps. Fire Mater 2023;47:415–32. https://doi.org/10.1002/fam.3121.

[13] Janssens ML. Modeling of the thermal degradation of structural wood members exposed to fire. Fire Mater 2004;28:199–207. https://doi.org/10.1002/fam.848.

[14] Ronquillo G, Hopkin D, Spearpoint M. Review of large-scale fire tests on cross-laminated timber. J Fire Sci 2021;39:327–69. https://doi.org/10.1177/07349041211034460.

[15] Schmidt L, Hadden RM, Fernando D. Observations and impact of char layer formation and loss for engineered timber. Fire Saf J 2024;147:104196. https://doi.org/10.1016/j.firesaf.2024.104196.

[16] Čolić A, Wiesner F, Hopkin D, Spearpoint M, Wu W, Bisby L. Application of microscale methods to study the heat-induced delamination in engineered wood products bonded with one-component polyurethane adhesives. Int J Adhes Adhes 2024;135:103834. https://doi.org/10.1016/j.ijadhadh.2024.103834.

[17] Nothard S, Lange D, Hidalgo JP, Gupta V, McLaggan MS, Wiesner F, et al. Factors influencing the fire dynamics in open-plan compartments with an exposed timber ceiling. Fire Saf J 2022;129:103564. https://doi.org/10.1016/j.firesaf.2022.103564.

[18] Kotsovinos P, Rackauskaite E, Christensen E, Glew A, O'Loughlin E, Mitchell H, et al. Fire dynamics inside a large and open-plan compartment with exposed timber ceiling and columns: *CodeRed #01*. Fire Mater 2023;47:542–68. https://doi.org/10.1002/fam.3049.

[19] Bøe AS, Friquin KL, Brandon D, Steen-Hansen A, Ertesvåg IS. Fire spread in a large compartment with exposed cross-laminated timber and open ventilation conditions: #FRIC-02 - exposed wall and ceiling. Fire Saf J 2023;141:103986. https://doi.org/10.1016/j.firesaf.2023.103986.

[20] Wiesner F, Xu H, Lange D, Gupta V, Pope I, Torero JL, et al. Large-scale compartment fires to develop a self-extinction design framework for mass timber-Part 2: Results, analysis and design implications. Fire Saf J 2025;152:104346. https://doi.org/10.1016/j.firesaf.2025.104346.

[21] Kotsovinos P, Christensen EG, Glew A, O'Loughlin E, Mitchell H, Amin R, et al. Impact of partial encapsulation on the fire dynamics of an open-plan compartment with exposed timber ceiling and columns: *CodeRed #04*. Fire Mater 2023;47:597–626. https://doi.org/10.1002/fam.3112.

[22] Gernay T, Zehfuß J, Brunkhorst S, Robert F, Bamonte P, McNamee R, et al. Experimental investigation of structural failure during the cooling phase of a fire: timber columns. Fire Mater 2023;47:445–60. https://doi.org/10.1002/fam.3110.

[23] F. Robert, J.-M. Franssen, J. Zehfuß, S. Brunkhorst, P. Bamonte, S. Renard, , Natural fire tests on GLT columns including the cooling down phase, in: World Conference on Timber Engineering (WCTE 2023), Oslo, Norway, 2023: pp. 1848–1854. https://doi.org/10.52202/069179-0244.

[24] Renard S, Robert F, Franssen J-M, Zehfuß J, McNamee R, Bamonte P, et al. Structural behavior of timber columns in wood crib compartment fire tests. Fire Saf J 2025:104413. https://doi.org/10.1016/j.firesaf.2025.104413.

[25] C. Douglas, D. Pau, D. Moroder, A. Buchanan, Structural design of timber columns in realistic fires, in: World Conference on Timber Engineering 2025, Brisbane, Australia, n.d.

[26] CEN, EN 14080: Timber structures – Glued laminated timber and glued solid timber – Requirements; 2013.

[27] CEN, Eurocode 1: Actions on structures - Part 1-1: General actions - Densities, self-weight, imposed loads for buildings; 2002.

[28] CEN, Eurocode 5 – Design of timber structures Part 1-2: General – Structural fire design; 2020.

[29] Franssen J-M, Gernay T. Modeling structures in fire with SAFIR®: theoretical background and capabilities. JSFE 2017;8:300–23. https://doi.org/10.1108/JSFE-07-2016-0010.
[30] CEN, Eurocode 5: Design of timber structures - Part 1-2: General - Structural fire design; 2004.
[31] Ma C, Garcia-Castillo E, Paya-Zaforteza I, Gernay T. Modeling fire resistance of timber columns: Influence of elevated-temperature material models in finite element analysis. Structures 2025;82:110629. https://doi.org/10.1016/j.istruc.2025.110629.
[32] CEN, Eurocode 5: Design of timber structures - Part 1-1: General - Common rules and rules for buildings; 2004.
[33] Garcia-Castillo E, Gernay T, Paya-Zaforteza I. Probabilistic models for temperature-dependent compressive and tensile strengths of timber. J Struct Eng 2023;149:04022239. https://doi.org/10.1061/JSENDH.STENG-11369.
[34] Mitchell H, Amin R, Heidari M, Kotsovinos P, Rein G. Structural hazards of smouldering fires in timber buildings. Fire Saf J 2023;140:103861. https://doi.org/10.1016/j.firesaf.2023.103861.
[35] Mindeguia J, Mohaine S, Bisby L, Robert F, McNamee R, Bartlett A. Thermo-mechanical behaviour of cross-laminated timber slabs under standard and natural fires. Fire Mater 2021;45:866–84. https://doi.org/10.1002/fam.2938.
[36] Kotsovinos P, Christensen EG, Rackauskaite E, Glew A, O'Loughlin E, Mitchell H, et al. Impact of ventilation on the fire dynamics of an open-plan compartment with exposed timber ceiling and columns: *CodeRed #02*. Fire Mater 2023;47:569–96. https://doi.org/10.1002/fam.3082.